

RESEARCH PAPER



Microbiota manipulation to increase macrophage IL-10 improves colitis and limits colitis-associated colorectal cancer

Daniel F. Zegarra Ruiz^a, Dasom V. Kim^{a,b}, Kendra Norwood^c, Fatima B. Saldana-Morales^{a,d}, Myunghoo Kim^{c+}, Charles Ng^e, Ryann Callaghan^b, Maisha Uddin^a, Lin-Chun Chang^a, Randy S. Longman^{f,g,h}, and Gretchen E. Diehl^{a,b}

^aImmunology Program, Memorial Sloan Kettering Cancer Center, New York, NY, USA; ^bImmunology and Microbial Pathogenesis Program, Weill Cornell Graduate School of Medical Sciences, New York, NY, USA; ^cDepartment of Molecular Virology and Microbiology, Baylor College of Medicine, Houston, TX, USA; ^dNeuroscience Program, Baylor College of Medicine, Houston, TX, USA; ^eDepartment of Pathology, Joan & Sanford I. Weill Medical College of Cornell University, New York, NY, USA; ^fDivision of Gastroenterology and Hepatology, Department of Medicine, Weill Cornell Medicine, New York, NY, USA; ^gJill Roberts Institute for Research in Inflammatory Bowel Disease, Weill Cornell Medicine, New York, NY, USA; ^hJill Roberts Center for Inflammatory Bowel Disease, Weill Cornell Medicine, New York, NY, USA

ABSTRACT

Inflammatory bowel disease (IBD) is a chronic life-long inflammatory disease affecting almost 2 million Americans. Although new biologic therapies have been developed, the standard medical treatment fails to selectively control the dysregulated immune pathways involved in chronic colonic inflammation. Further, IBD patients with uncontrolled colonic inflammation are at a higher risk for developing colorectal cancer (CRC). Intestinal microbes can impact many immune functions, and here we asked if they could be used to improve intestinal inflammation. By utilizing an intestinal adherent *E. coli* that we find increases IL-10 producing macrophages, we were able to limit intestinal inflammation and restrict tumor formation. Macrophage IL-10 along with IL-10 signaling to the intestinal epithelium were required for protection in both inflammation and tumor development. Our work highlights that administration of immune modulating microbes can improve intestinal outcomes by altering tissue inflammation.

ARTICLE HISTORY

Received 25 May 2022
Revised 18 August 2022
Accepted 25 August 2022

KEYWORDS

Microbiota; intestinal inflammation; colorectal cancer; colitis-associated cancer; *E. coli*; IL-10; intestinal macrophages; intestinal epithelium

Introduction

Inflammatory bowel disease (IBD), including Crohn's disease (CD) and ulcerative colitis (UC), is a chronic inflammatory intestinal disease with no cure¹. It affects almost 2 million people in the United States.² IBD is thought to result from unchecked inflammation against the microbiota in a genetically susceptible individual.³ Although new biologic therapies have been developed, the standard medical treatment fails to selectively control the dysregulated immune pathways involved in chronic colonic inflammation.⁴ In IBD patients, changes in the microbiota are found, including expanded pro-inflammatory microbes such as *Ruminococcus gnavus* and proteobacteria, such as *Escherichia coli* and reduced anti-inflammatory microbes such as Bacteroidetes, *Lachnospiraceae*, and *Faecalibacterium prausnitzii*.^{5–8} This altered microbiota is thought to support disease progression and inflammatory changes.⁹ In parallel, genetic, and

environmental factors can interfere with proper interaction between the host immune system and microbiota leading to enhanced inflammation.^{10,11}

IBD patients with poorly controlled intestinal inflammation are at an elevated risk for CRC development.^{10–13} Furthermore, chronic intestinal inflammation corresponds with advanced disease stage and decreased survival in CRC.^{14,15} Animal models support a causative role for inflammation in CRC with inflammation promoting tumorigenesis.¹⁴

Numerous groups find the microbiota can both enhance and limit intestinal inflammation. Specifically, we and others find that microbiota-derived signals drive anti-inflammatory processes including macrophage IL-10 production,¹⁶ induction of naive and regulatory T cells,^{17,18} and fortification of the epithelial barrier.^{19–21} We previously identified that colonization with

CONTACT Gretchen E. Diehl  diehlg1@mskcc.org  Immunology Program, Memorial Sloan Kettering Cancer Center, New York, NY, USA

⁺Current Address: Department of Animal Science, Pusan National University, Pusan, South Korea

 Supplemental data for this article can be accessed online at <https://doi.org/10.1080/19490976.2022.2119054>

© 2022 The Author(s). Published with license by Taylor & Francis Group, LLC.

This is an Open Access article distributed under the terms of the Creative Commons Attribution-NonCommercial License (<http://creativecommons.org/licenses/by-nc/4.0/>), which permits unrestricted non-commercial use, distribution, and reproduction in any medium, provided the original work is properly cited.

multiple human *E. coli* isolates could replace the microbiota in inducing macrophage IL-10 production, limiting pathology in a model of *Salmonella* infection¹⁶ but it remained unclear if such microbes could further enhance IL-10 and anti-inflammatory effects in the context of the normal microbiota.

Here, we find that colonization with the IL-10 inducing *E. coli*, strain 541-15, increased macrophage IL-10 production but only after intestinal damage. This increased IL-10 production after 541-15 colonization offered protection from intestinal injury as well as limited development of colitis-associated CRC (CAC). These data demonstrate that addition of select microbes is sufficient to shift immune function leading to improved outcomes in models of colitis, and offers insight into the role of gut microbes in intestinal inflammation and cancer.

Results

Intestinal colonization with *E. coli* 541-15 protects from colitis

As we previously found that colonization with *E. coli* 541-15 after microbiota depletion with antibiotics was sufficient to induce intestinal CX₃CR1⁺ macrophage production of IL-10 which restricted *Salmonella*-specific Th1 cells,¹⁶ we asked if 541-15 protected from intestinal injury and inflammation in the presence of the steady-state SPF microbiota. We left *E. coli*-free specific-pathogen-free (SPF) C57BL/6 (B6) mice uncolonized or colonized with *E. coli* 541-15 2 days before treatment with dextran sodium sulfate (DSS). In this acute intestinal inflammation model, DSS treatment causes epithelial damage and inflammation in the intestine.²² *E. coli* colonization was confirmed by qPCR using *E. coli* specific 16s rRNA primers (Figure S1A). *E. coli* 541-15 colonization did not alter the overall composition of the microbiome (Figures S1B-S1D). We found that colonization with *E. coli* 541-15 prevented weight loss and colon shortening, and improved histopathology with less incidence of ulcerations and fewer neutrophil clusters in lamina propria and epithelium (Figures 1A-1d). We also found decreased expression of pro-inflammatory markers lipocalin-2 and myeloperoxidase in fecal samples from *E. coli* 541-15 colonized mice as well as reduced expression of tumor necrosis factor alpha

supporting reduced colonic inflammation (Figures 1E, 1f and S1E). As intestinal inflammation is linked with increased gut permeability, we assayed for intestinal permeability after DSS treatment by gavaging mice with fluorescein isothiocyanate (FITC) conjugated dextran (FITC-dextran) and measuring serum FITC-dextran levels.²³ DSS-treated mice had increased serum FITC-dextran levels that were reduced in 541-15 colonized mice demonstrating decreased intestinal permeability (Figure 1g). Decreased permeability reflects improved intestinal barrier integrity, likely the consequence of lower intestinal inflammation and improved repair.²⁴⁻²⁶ We also characterized immune infiltration in DSS-treated *E. coli* 541-15 colonized mice. In the colon lamina propria, *E. coli* 541-15-colonized mice had decreased immune infiltration (Figure 1h) with decreased Th1 cells, CTLs, and neutrophils as well as increased Tregs and no change in macrophages or monocytes (Figures 1I-1m). Supporting these findings, in the mesenteric lymph node (MLN), *E. coli* 541-15-colonized mice had decreased IFN γ -producing CD4⁺ T cells and ILCs (Figure S1F). Our mice are segmented filamentous bacteria (SFB) free and so we do not see T helper 17 (Th17) cell responses, and these are not altered by 541-15 colonization (Figure S1F). To test if 541-15 enhanced IL-10 production in the presence of the SPF microbiota, we colonized *E. coli*-free SPF IL-10-GFP reporter mice (Vert-X) with 541-15 and left untreated or treated with 2% DSS for 7 days and used flow cytometry to detect IL-10⁺ cells.^{27,28} As previously described^{27,28} we find CX₃CR1⁺ macrophages to be the main source of IL-10 (Figure S2A). However, 541-15 colonization did not enhance IL-10 production in the presence of the SPF microbiota (Figure S2B). In contrast, after DSS treatment, we find increased IL-10⁺ cells in the colon of 541-15 colonized mice with increased IL-10 expression by CX₃CR1⁺ macrophages (Figures 2A and 2b).

Intestinal colonization with *E. coli* 541-15 prevents colitis by inducing IL-10 production by CX₃CR1⁺ macrophages which targets the intestinal epithelium

IL-10 deficient mice develop microbiota-driven spontaneous colitis and also show increased sensitivity to DSS.²⁹ To assess the requirement for IL-10 in colitis

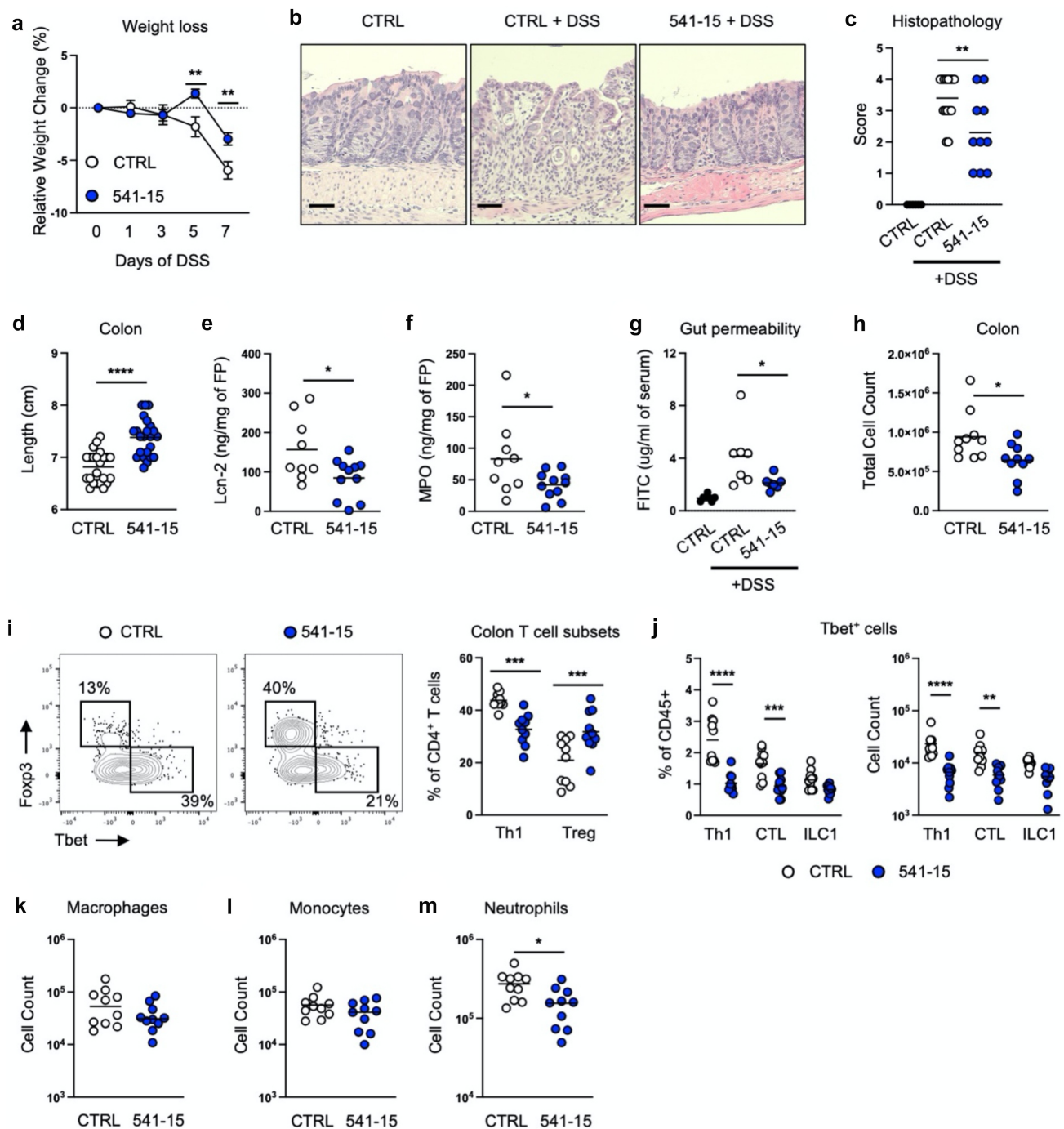


Figure 1. Intestinal colonization with *E. coli* 541-15 protects from colitis. Wildtype mice were colonized with *E. coli* 541-15 or gavaged with LB broth (CTRL) and 3 days later 2% DSS was provided in drinking water. At day 7 of DSS treatment, samples were collected. (a) Relative weight change. (b) Representative H&E staining of distal colons. Scale bars represent 50 μ m. (c) Histopathology scores. (d) Colon lengths. (e) Lipocalin-2 (Lcn-2) and (f) Myeloperoxidase (MPO) concentration in fecal pellets. At day 7 mice were gavaged with FITC-dextran and 3 hours later blood was collected. (g) FITC concentration in serum. Colon lamina propria cells were isolated. (h) Number of immune cells. (i) Flow cytometry and frequencies of Th1 and Tregs. (j) Frequencies and counts of total Th1 cells, CTLs, and ILC1s. Counts of (k) Macrophages, (l) Monocytes, and (m) Neutrophils. Each replicate is a biologically independent sample. Individual dots represent samples from individual mice. Data are shown as individual values and mean, compared by two-tailed unpaired t-test or two-way ANOVA with Fisher's LSD post hoc test. The results are representative of at least two independent experiments. * $P < .05$ was considered statistically significant; ** $P < .01$; *** $P < .001$; **** $P < .0001$. See also Figure S1.

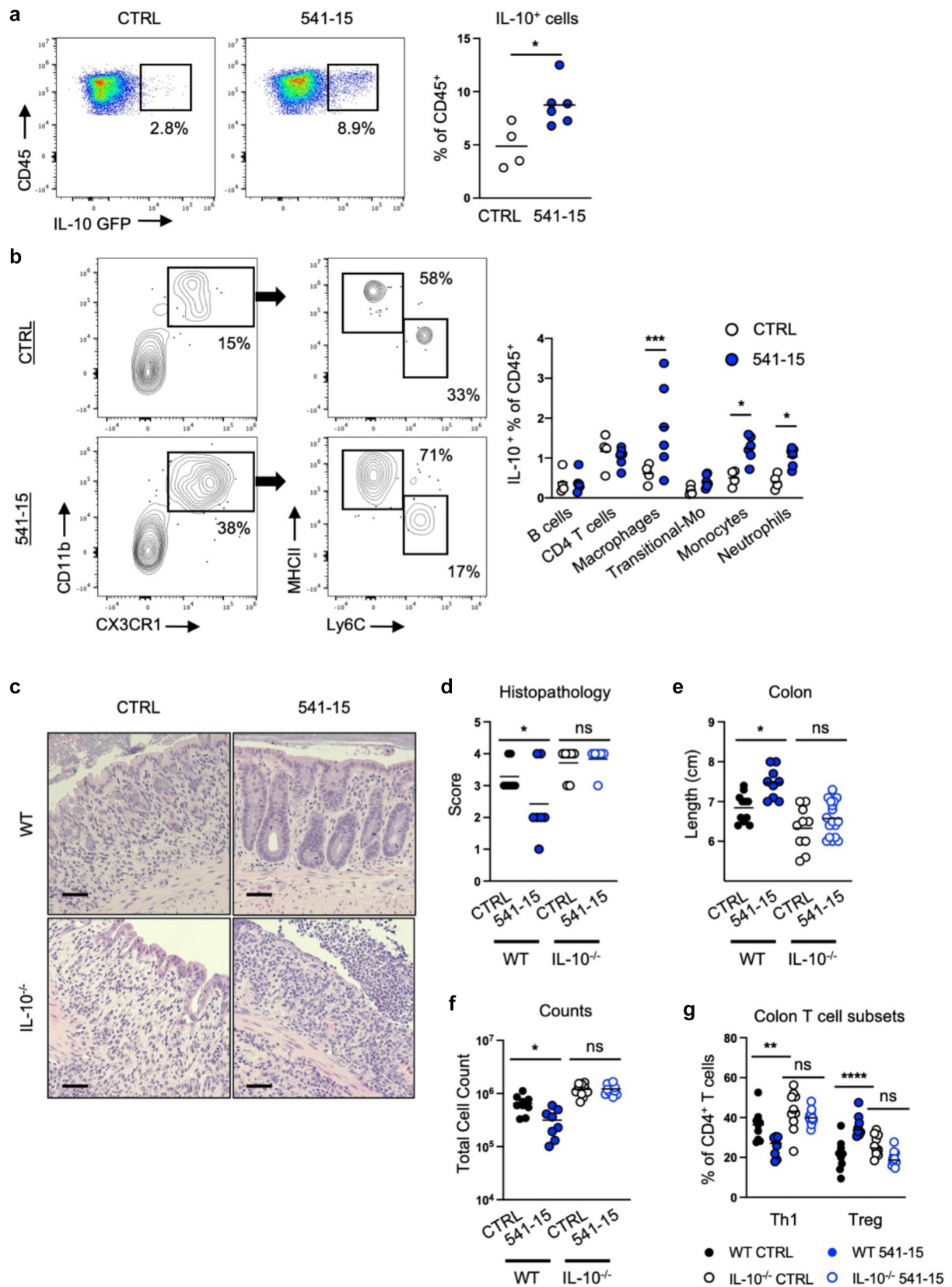


Figure 2. Intestinal colonization with *E. coli* 541-15 prevents colitis through IL-10 induction. Vert-X mice were colonized with *E. coli* 541-15 or gavaged with LB broth (CTRL) and 3 days later 2% DSS was provided. At day 7 of DSS treatment, samples were collected. Flow cytometry and frequencies of (a) total IL-10⁺ immune cells from the colonic lamina propria and (b) identification of IL-10⁺ immune cells. IL-10 deficient (IL-10^{-/-}) and wildtype (WT) littermate mice were colonized with *E. coli* 541-15 or gavaged with LB

protection downstream of 541–15 colonization, we left IL-10 wildtype and knockout (IL-10^{-/-}) littermate mice uncolonized or colonized with *E. coli* 541–15 before DSS treatment. As above, 541–15 colonization improved colitis in wildtype mice (Figures 2C–2g and S2C–S2H). However, in IL-10 knockout mice 541–15 colonization did not improve colitis outcomes including no effect on colon length, histopathology scores, or immune infiltration (Figures 2C–2g and S2C–S2H), supporting the requirement of IL-10 in protection after 541–15 colonization.

To assess the role of CX₃CR1⁺ macrophages in 541–15 protection from colitis, we used mice where the diphtheria toxin receptor (DTR) is expressed from the *Cx3cr1* locus (CX3-DTR mice).³⁰ In these mice, all CX₃CR1⁺ cells are depleted after diphtheria toxin (DT) injection. Colonization of these mice with 541–15 before DSS treatment did not induce changes in colon length or infiltrating immune cells (Figures S3A–S3D). This is likely because DT treatment depleted both CX₃CR1⁺ monocytes that drive pathology in colitis and CX₃CR1⁺ macrophages that are important for barrier repair.³¹ Therefore, we used mice where a floxed-stop cassette upstream of the DTR was inserted into the *Cx3cr1* locus (CX3-STOP-DTR). Crossing these mice to CD11c-Cre allows for depletion of CX₃CR1⁺ macrophages and dendritic cells (DCs) but not monocytes or other CX₃CR1-expressing cells after DT injection.³² After 541–15 colonization and DSS treatment, mice lacking CX₃CR1⁺ macrophages and DCs had shorter colons with increased immune infiltration including more Th1 cells, CTLs, ILC1s, and fewer Tregs as compared to littermate controls (Figures S3E–S3H).

We next used mice lacking IL-10 production by CX₃CR1⁺ cells to test if CX₃CR1⁺ cell IL-10 was required for colitis protection after *E. coli* 541–15 colonization. For these experiments, mice with a conditional allele for IL-10 were crossed to the tamoxifen-inducible CX₃CR1-CreERT2.³³ Tamoxifen treatment results in loss of IL-10 production by CX₃CR1⁺ cells in IL-10^{flox/-}

compared to IL-10^{flox/+} littermate control CX₃CR1-CreERT2 mice. As compared to controls, in DSS treated 541–15 colonized mice whose CX₃CR1⁺ cells cannot produce IL-10, we found loss of protection by *E. coli* 541–15 colonization with increased weight loss, shorter colon length, and increased pathology characterized by significant inflammatory infiltrate and ulcerations (Figures 3A–3c and S3I). We also found increased immune infiltration with increased Th1 cells, ILC1s, and neutrophils (Figures 3D, 3e, and S3J–S3L). In contrast, we found T cell IL-10 was dispensable as we found complete protection after 541–15 colonization of mice where T cells could not produce IL-10, with improved colon length and histopathology after 541–15 colonization (Figures S3M–S3R).

To identify the cellular target of CX₃CR1⁺ macrophage IL-10 after *E. coli* 541–15 colonization we next analyzed mice in which epithelial cells, CX₃CR1⁺ cells, or T cells lack expression of the IL-10 receptor α (IL-10 Ra). Suppression of colitis by *E. coli* 541–15 was intact when mice lacked IL-10Ra expression in T cells or CX₃CR1⁺ cells (Figures S4A–S4L). In contrast, we found epithelial IL-10Ra is required as 541–15 was no longer protective after DSS treatment in LGR5-CreERT2⁺ IL-10Ra^{flox/flox} mice as compared to littermates without LGR5-CreERT2, as seen by increased weight loss, shorter colon length, increased histopathology scores, and increased epithelial permeability (Figures 4A–4c, S4M, and S4N). In these mice we found increased immune infiltration with increased Th1 cells (Figures 4D, 4e, and S4O–S4Q). In addition, fecal lipocalin-2 and myeloperoxidase were increased in DSS-treated 541–15 colonized mice when epithelial cells lack IL-10Ra (Figures S4R and S4S). In epithelial cells, IL-10 triggers repair pathways including WNT signaling that leads to downstream expression of the pluripotency gene *nanog* which supports cell proliferation and epithelial barrier repair.^{34,35} Confirming the role of IL-10 in epithelial cells, we find that *E. coli*

broth (CTRL) and 3 days later 2% DSS was provided. At day 7 of DSS treatment, samples were collected. (c) Representative H&E staining of distal colons. Scale bars represent 50 μ m. (d) Histopathology scores. (e) Colon lengths. Colon lamina propria cells were isolated. (f) Number of immune cells. (g) Frequencies of Th1 and Tregs. Each replicate is a biologically independent sample. Individual dots represent samples from individual mice. Data are shown as individual values and mean, compared by two-tailed unpaired t-test or two-way ANOVA with Fisher's LSD post hoc test. The results are representative of at least two independent experiments. *P < .05 was considered statistically significant; **P < .01; ***P < .001; ****P < .0001. See also Figure S2.

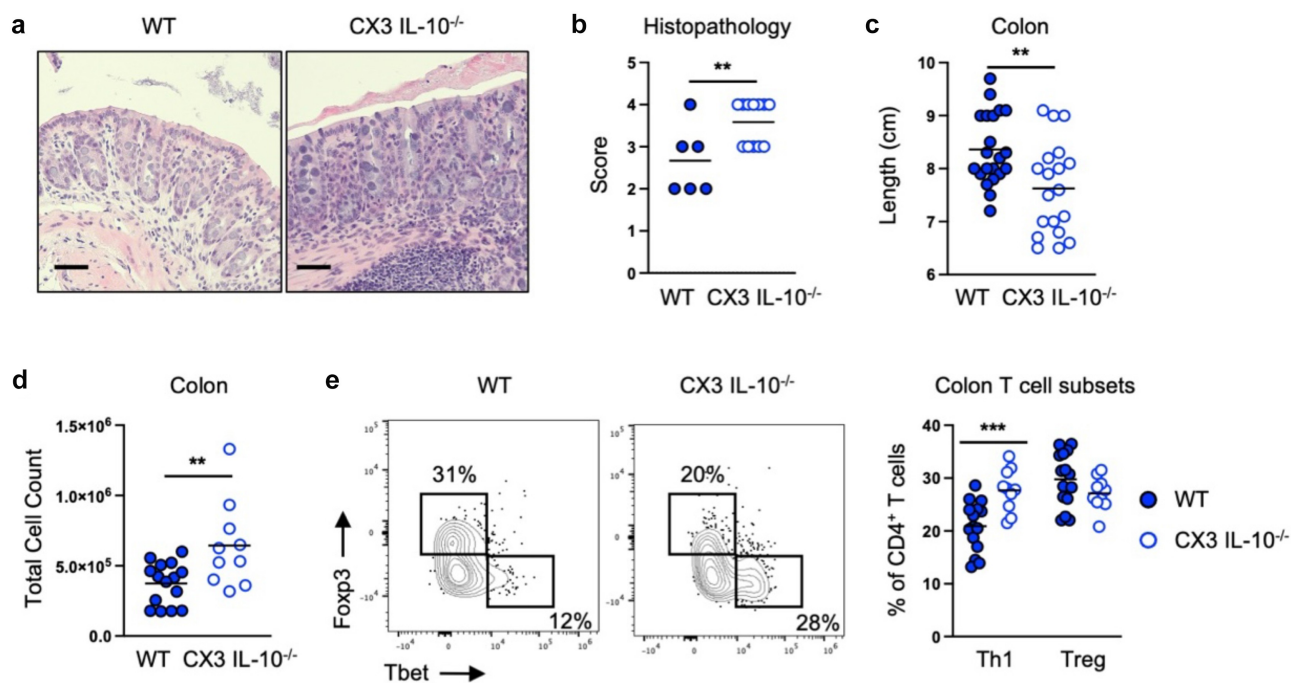


Figure 3. Intestinal colonization with *E. coli* 541–15 prevents colitis by inducing IL-10 production by CX3CR1+ macrophages. IL-10^{flx/-} (CX3 IL-10^{-/-}) and IL-10^{flx/+} (WT) littermate CX3CR1-CreERT2 mice were colonized with *E. coli* 541–15 and 3 days later 2% DSS was provided. At day 7 of DSS treatment, samples were collected. 3 days before colonization and every 2 days throughout the experiment 4OHT was injected to both groups. (a) Representative H&E staining of distal colons. Scale bars represent 50 μ m. (b) Histopathology scores. (c) Colon lengths. Colon lamina propria cells were isolated. (d) Number of immune cells. (e) Flow cytometry and frequencies of Th1 and Tregs. Each replicate is a biologically independent sample. Individual dots represent samples from individual mice. Data are shown as individual values and mean, compared by two-tailed unpaired t-test or two-way ANOVA with Fisher's LSD post hoc test. The results are representative of at least two independent experiments. * $P < .05$ was considered statistically significant; ** $P < .01$; *** $P < .001$. See also Figure S3.

541–15 colonization increased *nanog* expression in the colon of DSS-treated wild-type mice (Figure S4T).

Intestinal colonization with *E. coli* 541-15 protects from colitis-associated colorectal cancer

As intestinal inflammation is a risk for CAC development and dysbiosis characterized by enriched mucosa adherent bacteria such as *E. coli* is seen during inflammatory conditions in human IBD patients, in mouse IBD models, and in colon cancer,^{10,11} we asked if colonization with *E. coli* 541–15 modulated an inflammation-driven mouse model of CAC. 6-week-old *E. coli*-free SPF B6 mice were subjected to a chemically induced colitis associated carcinoma model. In this colon tumor model, mice are treated with azoxymethane (AOM), a mutagen, followed by three cycles of 2% DSS.³⁶ Under the AOM/DSS model, mice develop tumors in the distal colon as early as 1 week after the second cycle of DSS.³⁶ We

colonized mice with *E. coli* 541–15 before the first DSS administration and assessed tumor formation 4 weeks after the last DSS cycle (Figure S5A). As predicted from its anti-inflammatory effect,¹⁶ we found *E. coli* 541–15 was protective with reduced number and size of tubular adenomas (Figures 5A and 5b). Spleen size was also reduced indicating reduced systemic inflammation (Figure S5B).

We further assessed how 541–15 colonization affected the immune microenvironment within the tumors (tumor microenvironment, TME) and surrounding tissue. Using flow cytometry, we found decreased infiltration of myeloid cells including tumor associated macrophages (TAMs), mononuclear myeloid-derived suppressor cells (M-MDSCs), and polymorphonuclear myeloid-derived suppressor cells (PMN-MDSCs) in tumors of mice colonized with 541–15 (Figures 5C and S5C). TAMs both inhibit anti-tumor T cell responses and directly promote tumor growth and angiogenesis.³⁷ M-MDSCs resemble monocytes while PMN-

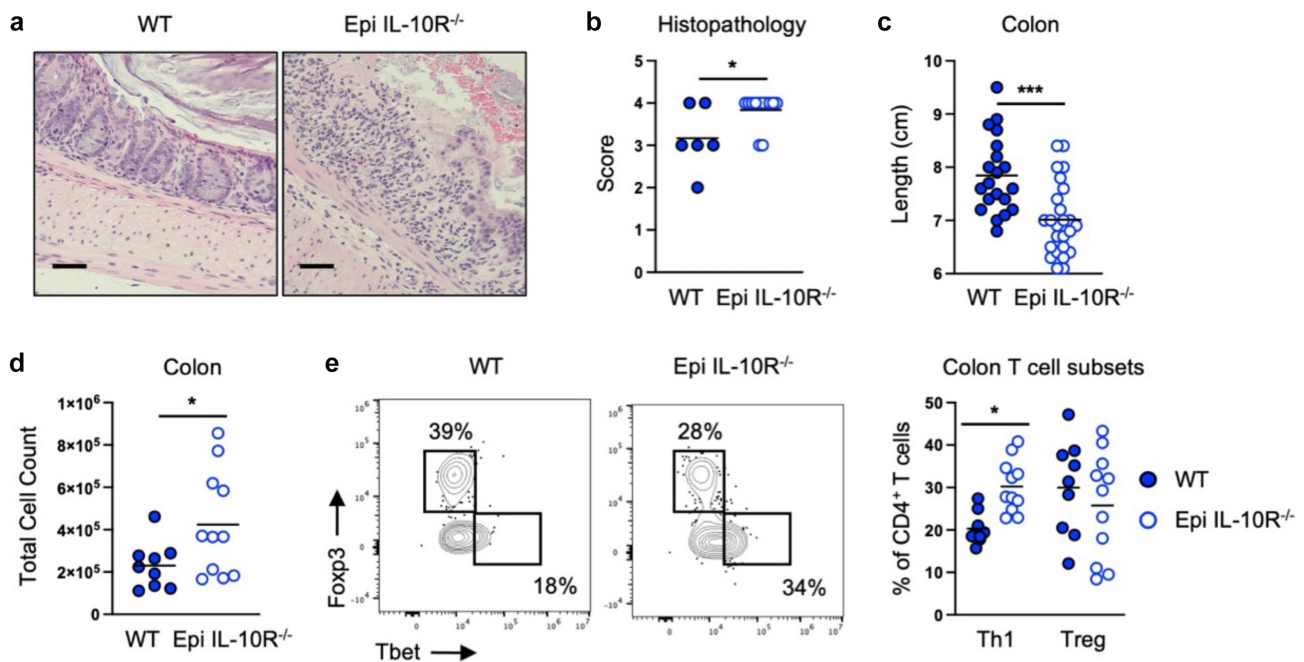


Figure 4. Intestinal colonization with *E. coli* 541–15 prevents colitis by modulating IL-10 signaling to intestinal epithelium. LGR5-CreERT2+ (Epi IL-10R^{-/-}) and LGR5-CreERT2- (WT) littermate IL-10Raflox/flox mice were colonized with *E. coli* 541–15 and 3 days later 2% DSS was provided. At day 7 of DSS treatment, samples were collected. 7 days before colonization 4OHT was injected on two consecutive days to both groups. (a) Representative H&E staining of distal colons. Scale bars represent 50 μ m. (b) Histopathology scores. (c) Colon lengths. Colon lamina propria cells were isolated. (d) Number of immune cells. (e) Flow cytometry and frequencies of Th1 and Tregs. Each replicate is a biologically independent sample. Individual dots represent samples from individual mice. Data are shown as individual values and mean, compared by two-tailed unpaired t-test or two-way ANOVA with Fisher's LSD post hoc test. The results are representative of at least two independent experiments. * $P < .05$ was considered statistically significant; *** $P < .001$. See also Figure S4.

MDSCs are similar to neutrophils and both inhibit T cell recruitment and suppress T cell responses within the tumor.^{38,39} We also found changes in recruitment of lymphoid cells to tumors in 541–15 colonized mice. As compared to control mice, mice colonized with *E. coli* 541–15 had increased T helper 1 (Th1) cells, cytotoxic T lymphocytes (CTLs), and type 1 innate lymphoid cells (ILC1s), and decreased regulatory T cells (Tregs) within tumors (Figures S5D and S5E). This shift in immune infiltration supports that 541–15 is restricting tumor development as smaller, better controlled tumors have increased T effector cells as compared to Tregs and MDSCs.³⁷ In contrast to tumor tissue, in tumor adjacent colonic tissue from 541 to 15 colonized mice we found the opposite effects with decreased Th1 cells and increased Tregs as compared to uncolonized mice (Figure S5F). This indicated 541–15 induced tumor-specific changes in infiltrating immune populations. Interestingly, as in DSS-induced colitis, *E. coli* 541–15 colonization did not

alter microbiota composition in mice under the CAC model (Figures S6A and S6B). This indicated that immune changes leading to protection against CAC were specific for 541–15 and is not attributed to changes in other microbial populations.

***E. coli* 541–15 modulates tumorigenesis through intestinal epithelium responses to IL-10 production from CX₃CR1⁺ macrophages**

We next assessed if colonization with *E. coli* 541–15 prevented CAC through the same pathways through which it protected from intestinal inflammation. IL-10^{flox/+} and IL-10^{flox/-} CX₃CR1-CreERT2 mice under the AOM/DSS model were colonized with 541–15 and concomitantly treated with tamoxifen (Figure S6C). Loss of CX₃CR1⁺ cell IL-10 during DSS treatment in the presence of *E. coli* 541–15 led to increased tumor number and size likely due to increased inflammation as described above (Figure S6E). No change in

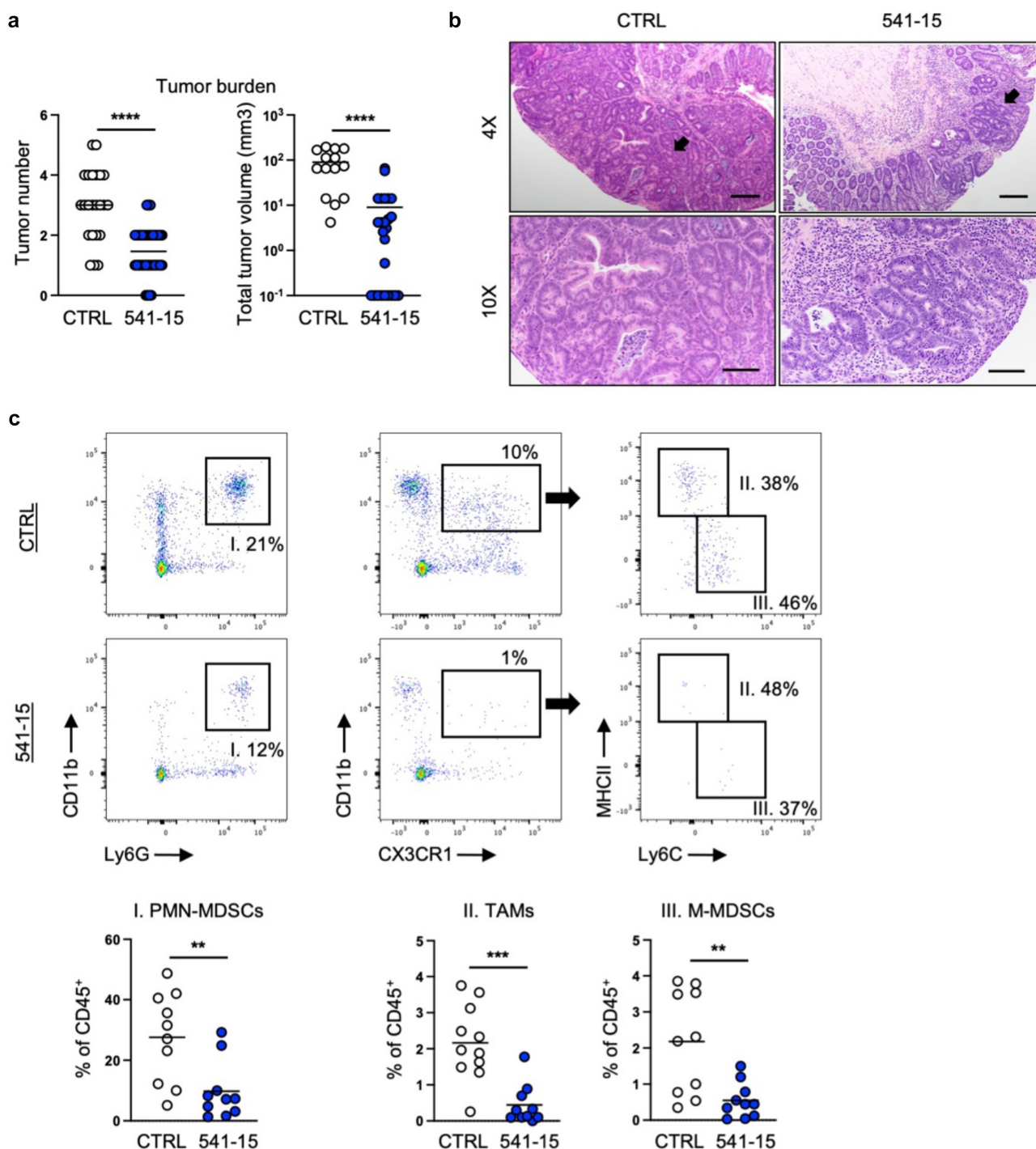


Figure 5. Intestinal colonization with *E. coli* 541-15 protects from colitis-associated colorectal cancer. Wildtype mice were administered AOM followed by 3 cycles of 2% DSS. Before administration of DSS mice were colonized with *E. coli* 541-15 or gavaged with LB broth (CTRL) and samples were collected as indicated in Figure S1A. (a) Number and size of colonic tumors. (b) Representative H&E staining of distal colons. Black arrow shows a tubular adenoma. Scale bars represent 4x = 200 μ m and 10x = 100 μ m. Tumors were individually collected, digested, and the tumor microenvironment was analyzed by flow cytometry. (c) Flow cytometry and frequencies of PMN-MDSCs, TAMs, and MMDSCs. Each replicate is a biologically independent sample. Individual dots represent samples from individual mice. Data are shown as individual values and mean, compared by two-tailed unpaired t-test. The results are representative of at least two independent experiments. * $P < .05$ was considered statistically significant; ** $P < .01$; *** $P < .001$; **** $P < .0001$. See also Figures S5 and S6.

tumor number or size was observed in mice lacking IL-10 production by T cells colonized with 541–15 (Figure S6E).

To assess the role of epithelial IL-10 signaling in *E. coli* 541–15 modulation of tumorigenesis, we used mice in which epithelial cells are deficient for IL-10R α after treatment with tamoxifen. IL-10R $\alpha^{\text{flox/flox}}$ mice with and without LGR5-CreERT2 were colonized with 541–15 and simultaneously treated with tamoxifen followed by treatment with AOM/DSS (Figure S6D). Similar to mice in which CX₃CR1⁺ cells do not produce IL-10, 541–15 colonized mice lacking epithelial IL-10R α had more frequent, larger tumors (Figure S6E). We saw no change in tumor number or size when CX₃CR1⁺ or T cells lacked IL-10R α (Figure S6E).

These results identify that microbiota modulation of macrophage anti-inflammatory function has direct outcomes on inflammation and CAC development. IL-10 produced primarily by CX₃CR1⁺ macrophages is sensed by epithelial cells potentially triggering epithelial repair processes helping in the resolution of inflammation and protecting from tumor development³⁴ (Figure S7A).

Discussion

Understanding the role of tissue inflammation is crucial to preventing and treating IBD, a chronic disease linked with changes in the gut microbial landscape that are thought to drive pathogenesis.^{5–9} Here, we find that colonization with a specific intestinal microbe restricts inflammation in a macrophage-dependent manner.

We and others previously demonstrated that the intestinal microbiota is a key regulator of intestinal macrophage inflammatory potential with the microbiota required for IL-10 production by intestinal macrophages.¹⁶ Particularly, we demonstrated that colonization with *E. coli* 541–15 was sufficient to restore CX₃CR1⁺ macrophage IL-10 production in microbiota depleted mice.¹⁶ Here, we find that 541–15 reduces intestinal pathology after DSS treatment. 541–15 colonization followed by DSS treatment results in enhanced macrophage IL-10 in the presence of the normal microbiota. Macrophage IL-10 production is required for protection as 541–15 is unable to protect from pathology in IL-10 deficient mice or in mice lacking IL-10

production by CX₃CR1⁺ macrophages. This confirms a critical role for microbial regulation of macrophage IL-10 in controlling intestinal inflammation.

We also find that intestinal epithelial cell response to IL-10 was required downstream of 541–15 colonization. In epithelial cells, IL-10 triggers repair pathways including WNT signaling pathways that support epithelial barrier repair further limiting tissue inflammation.^{34,35} Together, colonization with 541–15 protected from colitis only when intestinal epithelial cells were able to sense IL-10, highlighting the importance of crosstalk between macrophages and epithelial cells to support recovery from epithelial injury.

We next asked how this shift toward barrier support by 541–15 colonization regulated tumor development in a CAC model. In CRC, evidence supports that increased intestinal inflammation enhances intestinal tumors,^{40,41} likely driven by environmental and lifestyle changes that can interfere with proper host–microbiota interactions, leading to unresolved damage and unchecked inflammation that promotes CRC.¹³ In inflammatory disease, changes in microbiota composition can lead to lost regulatory capacity including decreased IL-10 production, that promotes or sustains inflammation.^{16,42,43} Recent studies identify select microbes as increased in CRC.^{10,11} One bacterium associated with worse CRC outcome is the attaching bacterium *Fusobacterium nucleatum*,¹⁰ which induces cell proliferation and modulation of the tumor microenvironment without altering inflammation.⁴⁴ We find that enrichment of *E. coli* 541–15, an adherent *E. coli* isolated from the intestine of an IBD patient,^{45,46} also affects CRC. However, contrary to *F. nucleatum*, 541–15 limits tumorigenesis by engaging IL-10 signaling pathways that suppress inflammation. Macrophages are known to produce additional factors that can promote tumor development. This includes transforming growth factor β 1 (TGF- β 1), insulin-like growth factor 1 (IGF-1), and vascular endothelial growth factor α (VEGF- α), which promote cellular proliferation and blood-vessel development.⁴⁷ It remains to be seen if 541–15 activates these pathways in addition to IL-10. As predicted by its ability to promote macrophage IL-10, colonization with 541–15 before induction of colitis in the mouse model of CAC led to reduced tumor incidence with fewer, smaller tumors in colonized mice. As in colitis, decreased tumorigenesis depended on

intestinal macrophage IL-10 production and IL-10 sensing by the intestinal epithelium.^{34,35}

Our findings suggest that modulating the function of CX₃CR1⁺ macrophages represents a therapeutic avenue to decrease inflammation that can lead to CAC in IBD patients.^{48,49} Although targeting specific microbes may offer therapeutic advantages, much work remains to be done to better characterize IBD-associated microbes and the downstream pathways they activate. Further studies should assess if using probiotics with immunomodulatory properties have therapeutic potential that provides protection against IBD and IBD-related cancer.

Materials and methods

Mice

All mice were bred in house at the animal facility of Baylor College of Medicine or Memorial Sloan Kettering Cancer Center and maintained as *E. coli* free. The colony is routinely tested by qPCR and immunophenotyping to confirm lack of *E. coli* colonization. C57BL/6 J (Jax #000664), IL10-GFP (Vert-X) (JAX #014530), IL-10KO (JAX #003968), CD11c-Cre (JAX #008068), LRG5-CreERT2 (JAX# 008875), CX₃CR1-CreERT2 (JAX #021160),³³ and CD4-Cre (JAX #017336), mice were originally purchased from Jackson laboratory before being bred in house. CX₃CR1-STOP-DTR (JAX #025629),³² CX₃CR1-DTR,³⁰ IL-10 flox,⁵⁰ and IL-10R α flox⁵¹ were previously described. See also Table S1. All mice were crossed at least 12 generations to the C57BL/6 J background. All mouse experiments were performed with mice between 6–20 weeks of age with males and females at similar ratios, unless otherwise specified. Littermate controls were used for each experiment, and mice were randomly assigned to experimental groups. All experiments were performed in accordance with approved protocols by the Institutional Animal Care and Usage Committee at Baylor College of Medicine and Memorial Sloan Kettering Cancer Center.

Induction of colitis and colonic tumors

Induction of colitis was performed by administering dextran sulfate sodium salt (DSS, mol wt 40

kDa; Alfa Aesar).²² Mice were administered 2% DSS in their drinking water for 7 days. Mice were weighed daily and analyzed after 7 days of DSS. For induction of colonic tumors, mice received a single injection of azoxymethane (AOM, Sigma) at 10 mg/kg body weight intraperitoneally. One week later, mice were treated with 3 cycles of 2% DSS (7 days) followed by 7 days of regular water. 4–5 weeks after the last cycle of DSS mice were analyzed.³⁶

Colonization of mice with *E. coli*

E. coli (EC) 541–15 was cultured overnight in LB media. Mice with a SPF microbiota were colonized with a single gavage of 10⁸ CFU of mouse commensal *E. coli*. Colonization was confirmed by qPCR with *E. coli*-specific primers using 16S (for fecal pellets) as housekeeping gene. Primers used were: 16S F: CGGTGAATACGTYCGG, 16S R: GGWTACCTTGTTACGACTT,⁵² *E. coli* F: GGTAGAGCACTGTTTTGGCA, *E. coli* R: TGTCTCCCGTGATAACTTTCT.⁵³

Diphtheria toxin (DT) and 4-hydroxytamoxifen (4OHT) administration

Mice were injected every other day with 200ng diphtheria toxin (DT, Sigma) in PBS. (Z)-4-Hydroxytamoxifen, 98% Z isomer (4OHT, Sigma) was resuspended to 20 mg/ml in ethanol by heating to 37°C. 4OHT was then diluted in corn oil (Sigma) to 2 mg/ml and mice were injected every 3 days with 100ul. All injections were intraperitoneal.

In vivo gut permeability assay with Fluorescein isothiocyanate (FITC)-dextran

Mice were weighed and fasted for 3 hours prior to oral FITC-dextran (4 kDa, Sigma) administration. A total concentration of 250 mg/kg body weight was administered through gavage. 3 hours after administration, blood samples were collected through retro-orbital bleeding and 50 ul of serum was placed in a fluorescence plate reader to determine the concentration by fluorescence excitation at 495 nm/519 nm reference.

DNA isolation and real-Time quantitative PCR (qPCR) analysis

For bacterial DNA identification, fecal pellets were collected and stored at -80°C . DNA was isolated using the DNeasy PowerSoil Kit according to the manufacturer's protocol (Qiagen). Real-time qPCR was performed using SYBR Green Supermix (Bio-Rad Laboratories) in the Bio-Rad thermocycler 384 well plates. Thermocycling program was 40 cycles at 95°C for 15s, 60°C for 30s, and 72°C for 30s, with an initial cycle of 95°C for 120s. Primers used were described above. Relative expression of target gene was determined using a standard curve to calculate the number of nucleotides per sample and the $\Delta\Delta\text{CT}$ method.

Cell isolation

Intestinal lamina propria cells were isolated as previously described.^{16,32,54} Briefly, mouse large intestines were washed in PBS, once with freshly prepared 30 mM EDTA and 1 mM DTT and once with 30 mM EDTA (both at 37°C), and then digested at 37°C in collagenase 8 (100 U/ml, Sigma) and DNase-containing (150 $\mu\text{g}/\text{ml}$, Sigma) media with 10% fetal bovine serum. Digested material was separated on a 40%/80% Percoll (GE Health) gradient. Tumors were digested as above, washed in PBS, and passed through a 40 μm strainer.

Antibodies, cell staining, and flow cytometry

Cells isolated from colon lamina propria and tumors were blocked with CD16/32 (Fc receptor) to prevent nonspecific antibody binding. Then, cells were surface-stained in FACS buffer (PBS, 2 mM EDTA, 2% fetal bovine serum) for 30 minutes in the dark at 4°C with fluorescently conjugated antibodies from BD, eBiosciences, or BioLegend specific to CD45 (30-F11), TCR β (H57-597), CD11b (M1/70), CD11c (N418), MHCII (M5/114.15.2), Ly6C (AL-21), CX3CR1 (SA011 F11), Ly6G (1A8), B220 (RA3-6B2), CD3 (145-2C11), CD90.2 (53-2.1), CD4 (GK1.5), and CD8 (53-6.7). For T cell subsets identification, after staining for surface antigens, cells were fixed and permeabilized using a Fixation/Permeabilization Solution

Kit (ThermoFisher) overnight at 4°C and stained with antibodies specific to mouse FOXP3 (FJK-16s) or T-bet (4B10) for 45 minutes at room temperature. To assess cytokine production after ex vivo restimulation, single-cell suspensions from mesenteric lymph nodes were incubated for 4 hours at 37°C with 5% CO_2 in the presence of 50 ng/mL PMA and 500 ng/mL ionomycin with 2 μM monensin (BD Biosciences). Flow cytometric analysis was performed on an LSR II (BD Biosciences) or Aurora (Cytek) and analyzed using FlowJo software (Tree Star Inc.). DAPI or live/dead fixable blue dead cell stain kit (ThermoFisher) was used to exclude dead cells. Total cell counts were determined with Precision Count Beads (BioLegend). Gating strategy is shown in Figure S5C. PMN-MDSCs were $\text{CD11b}^+\text{Ly6G}^+$, TAMs were $\text{CD11b}^+\text{CX}_3\text{CR1}^+\text{MHCII}^+\text{Ly6C}^-$, M-MDSCs were $\text{CD11b}^+\text{CX}_3\text{CR1}^+\text{MHCII}^-\text{Ly6C}^+$, Th1 cells were $\text{CD3}^+\text{TCR}\beta^+\text{CD4}^+\text{CD8}^-\text{Tbet}^+$, CTLs were $\text{CD3}^+\text{TCR}\beta^+\text{CD4}^-\text{CD8}^+\text{Tbet}^+$, ILC1s were $\text{CD3}^-\text{TCR}\beta^-\text{CD90.2}^+\text{Tbet}^+$, and Tregs were $\text{CD3}^+\text{TCR}\beta^+\text{CD4}^+\text{CD8}^-\text{Foxp3}^+$. All antibody information is listed below:

Antibody, Fluorochrome, Clone	Source	Catalog number
Anti-mouse MHCII (I-A/I-E), Pacific blue, clone M5/114.15.2	BioLegend	Cat# 107,620
Anti-mouse CD11c, PEcy7, clone N418	BioLegend	Cat# 117,317
Anti-mouse/human CD11b, APC/Cy7, clone M1/70	BioLegend	Cat# 101,226
Anti-mouse CX ₃ CR1, FITC, clone SA011 F11	BioLegend	Cat# 149,020
Anti-mouse Ly6C, Alexa Fluor 700, clone AL-21	BD	Cat# 561,237
Anti-mouse Ly6G, PE, clone 1A8	BioLegend	Cat# 127,608
Anti-mouse CD4, Brilliant Violet 510, clone GK1.5	BioLegend	Cat# 100,449
Anti-human/mouse T-bet, PEcy7, clone 4B10	eBiosciences	Cat# 25-5825-82
Anti-mouse CD3, APC/Cy7, clone 145-2C11	BioLegend	Cat# 100,330
Anti-mouse TCR β , Percp/Cy5.5, clone H57-597	BioLegend	Cat# 109,228
Anti-mouse/rat Foxp3, eFluor660, clone FJK-16s	eBiosciences	Cat# 50-5773-82
Anti-mouse CD45, Brilliant Violet 785, clone 30-F11	BioLegend	Cat# 103,149
Anti-human/mouse B220, Brilliant Violet 650, clone RA3-6B2	BioLegend	Cat# 103,241
Anti-mouse CD90.2, BUV395, clone 53-2.1	BD	Cat# 565,257
Anti-mouse CD8, APC, clone 53-6.7	BioLegend	Cat# 100,712
Anti-mouse IFN γ , FITC, clone XMG1.2	BioLegend	Cat# 505,806
Anti-mouse IL-17A, BV421, clone TC11-18H10.1	BioLegend	Cat# 506,926

Enzyme-linked immunosorbent assays (ELISAs)

Fecal lipocalin-2 (Lcn-2) and myeloperoxidase (MPO) were determined by ELISA (R&D Systems). Fecal samples were solubilized in PBS with protease inhibitors at 10 mg/100 μ l using a Mixer Mill.

Histology

Distal colons were fixed in 10% neutral buffered formalin, routinely processed, sectioned at 6 mm, and stained with hematoxylin and eosin (H&E) for light microscopic examination. Images were taken at 40X or 100X magnification using a ZEISS Axio Observer 2. Samples were assessed in a blinded fashion and scored 0 to 4 based on the criteria previously described:⁵⁵ (grade 0) Minimal chronic inflammatory infiltrate; (grade 1) Chronic inflammatory infiltrate; (grade 2) Few or rare neutrophils in lamina propria or epithelium; (grade 3) Multiple clusters of neutrophils in lamina propria and/or epithelium; (grade 4) Ulceration.

16S rDNA high-Throughput sequencing

Mouse fecal samples were collected sterilely and stored at -80° C. DNA was extracted utilizing Promega Max Prep & Promega Maxwell RSC 48 Instrument. The V4 and V5 regions of the 16S rDNA were PCR amplified, normalized, pooled, and sequenced using the Illumina MiSeq platform with 2×300 bp paired end reads. Analysis of 16S rDNA sequencing reads was performed using the software USEARCH (version 11.0.667) assigning taxonomy using the RDP 16S training set (version 16) as reference database. Merge reads with an expected error number over 1.0 were filtered. Filtered operational taxonomic units (OTUs) were rarefied to a depth of 17,481 reads per sample. Extraction, sequencing, and data processing were performed by the Microbiome Core Lab of Weill Cornell Medicine.

Statistics and reproducibility

Statistical analysis was performed using GraphPad Prism. All data are presented as individual values and mean. Two-tailed unpaired Student's t-test using a 95% confidence interval was used to evaluate the difference between two groups. For more than

two groups, One-way ANOVA was used. For more than two groups under different conditions Two-way ANOVA was used. A probability value of $p < .05$ was considered significant. Statistical significance is indicated in each figure. Each experiment was repeated independently at least 2 times with similar results. Representative flow plots and micrographs were selected from the pool of biological replicates indicated in their respective quantifications.

Acknowledgments

We thank all members of the Diehl and Longman labs for their critical input on the manuscript.

Disclosure statement

The authors declare no conflict of interests.

Funding

This work was supported by the NIH AI125264 (G.E.D.), Rainin Foundation (G.E.D.), Ludwig Center at Memorial Sloan Kettering (D.F.Z.), AAI Careers in Immunology Fellowship (M.K.), MSK Cancer Center Core Grant (P30 CA 008748), the Cytometry and Cell Sorting Core at Baylor College of Medicine (P30 AI036211, P30 CA125123, and S10 RR024574), and the Microbiome Core Lab of Weill Cornell Medicine; Ludwig Family Foundation;

ORCID

Gretchen E. Diehl  <http://orcid.org/0000-0002-1841-2842>

Contributions

D.F. Zegarrra-Ruiz, R.S. Longman, and G.E. Diehl designed the experiments and analyzed data. D.F. Zegarrra-Ruiz and G.E. Diehl wrote the manuscript with input from all co-authors. D. F. Zegarrra-Ruiz, D.V. Kim, K. Norwood, F.B. Saldana-Morales, M. Kim, C. Ng, R. Callaghan, M. Uddin, L. Chang, and G.E. Diehl conducted experiments and analyzed data.

Data availability

The authors confirm that the data supporting the findings of this study are available within the article and/or its supplementary materials. 16S sequencing data are openly available in NCBI under BioProject ID PRJNA845002.

References

- Baumgart DC, Carding SR. Inflammatory bowel disease: cause and immunobiology. *Lancet*. 2007;369(9573):1627–1640. doi:10.1016/S0140-6736(07)60750-8.
- Alatab S, Sepanlou SG, Ikuta K, Vahedi H, Bisignano C, Safiri S, Sadeghi A, Nixon MR, Abdoli A, Abolhassani H, et al. The global, regional, and national burden of inflammatory bowel disease in 195 countries and territories, 1990–2017: a systematic analysis for the global burden of disease study 2017. *Lancet Gastroenterology Hepatology*. 2020;5:17–30. doi:10.1016/S2468-1253(19)30333-4.
- Caruso R, Lo BC, Núñez G. Host–microbiota interactions in inflammatory bowel disease. *Nat Rev Immunol*. 2020;20:411–426. doi:10.1038/s41577-019-0268-7.
- Pithadia AB, Jain S. Treatment of inflammatory bowel disease (IBD). *Pharmacol Rep*. 2011;63:629–642. doi:10.1016/S1734-1140(11)70575-8.
- Dalal SR, Chang EB. The microbial basis of inflammatory bowel diseases. *J Clin Investigation*. 2014;124:4190–4196. doi:10.1172/JCI72330.
- Frank DN, Amand ALS, Feldman RA, Boedeker EC, Harpaz N, Pace NR. Molecular-phylogenetic characterization of microbial community imbalances in human inflammatory bowel diseases. *Proc National Acad Sci*. 2007;104:13780–13785. doi:10.1073/pnas.0706625104.
- Peterson DA, Frank DN, Pace NR, Gordon JI. Metagenomic approaches for defining the pathogenesis of inflammatory bowel diseases. *Cell Host Microbe*. 2008;3:417–427. doi:10.1016/j.chom.2008.05.001.
- Wu W-JH, Zegarra-Ruiz DF, Diehl GE. Intestinal microbes in autoimmune and inflammatory disease. *Front Immunol*. 2020;11:597966. doi:10.3389/fimmu.2020.597966.
- Elson CO, Cong Y. Host-microbiota interactions in inflammatory bowel disease. *Gut Microbes*. 2012;3:332–344.
- Sears CL, Garrett WS. Microbes, microbiota, and colon cancer. *Cell Host Microbe*. 2014;15(3):317–328. doi:10.1016/j.chom.2014.02.007.
- Chen J, Pitmon E, Wang K. Microbiome, inflammation and colorectal cancer. *Semin Immunol*. 2017;32:43–53. doi:10.1016/j.smim.2017.09.006.
- Longo DL, Beaugerie L, Itzkowitz SH, Longo DL. Cancers complicating inflammatory bowel disease. *New Engl J Medicine*. 2015;372:1441–1452. doi:10.1056/NEJMra1403718.
- Elinav E, Nowarski R, Thaïss CA, Hu B, Jin C, Flavell RA. Inflammation-induced cancer: crosstalk between tumours, immune cells and microorganisms. *Nat Rev Cancer*. 2013;13:759–771. doi:10.1038/nrc3611.
- Grivennikov SI, Greten FR, Karin M. Immunity, Inflammation, and Cancer. *Cell*. 2010;140:883–899. doi:10.1016/j.cell.2010.01.025.
- Siegel RL, Miller KD, Sauer AG, Fedewa SA, Butterly LF, Anderson JC, Cercek A, Smith RA, Jemal A. Colorectal cancer statistics, 2020. *Ca Cancer J Clin*. 2020;70:145–164. doi:10.3322/caac.21601.
- Kim M, Galan C, Hill AA, W-J W, Fehlner-Peach H, Song HW, Schady D, Bettini ML, Simpson KW, Longman RS, et al. Critical role for the microbiota in CX3CR1+ intestinal mononuclear phagocyte regulation of intestinal T cell responses. *Immunity* [Internet]. Available from. 2018;49:151–163.e5. <https://linkinghub.elsevier.com/retrieve/pii/S1074761318302450>
- Zegarra-Ruiz DF, Kim DV, Norwood K, Kim M, W-JH W, Saldana-Morales FB, Hill AA, Majumdar S, Orozco S, Bell R, et al. Thymic development of gut-microbiota-specific T cells. *Nature*. 2021;594:413–417. doi:10.1038/s41586-021-03531-1.
- Atarashi K, Tanoue T, Shima T, Imaoka A, Kuwahara T, Momose Y, Cheng G, Yamasaki S, Saito T, Ohba Y, et al. Induction of colonic regulatory T Cells by indigenous clostridium species. *Science*. 2011;331:337–341. doi:10.1126/science.1198469.
- Kamada N, Seo S-U, Chen GY, Núñez G. Role of the gut microbiota in immunity and inflammatory disease. *Nat Rev Immunol*. 2013;13:321–335. doi:10.1038/nri3430.
- Round JL, Mazmanian SK. The gut microbiota shapes intestinal immune responses during health and disease. *Nat Rev Immunol*. 2009;9:313–323. doi:10.1038/nri2515.
- Rakoff-Nahoum S, Paglino J, Eslami-Varzaneh F, Edberg S, Medzhitov R. Recognition of commensal microflora by toll-like receptors is required for intestinal homeostasis. *Cell*. 2004;118:229–241. doi:10.1016/j.cell.2004.07.002.
- Chassaing B, Aitken JD, Malleshappa M, Vijay-Kumar M. Dextran sulfate sodium (DSS)-induced colitis in mice. *Curr Protoc Immunol*. 2014;104:15.25.1–15.25.14.
- B-R L, Wu J, H-S L, Jiang Z-H, Zhou X-M, C-H X, Ding N, Zha J-M, W-Q H. In vitro and in vivo approaches to determine intestinal epithelial cell permeability. *J Vis Exp*. 2018. doi:10.3791/57032.
- Zegarra-Ruiz DF, Beidaq AE, Iñiguez AJ, Ricco MLD, Vieira SM, Ruff WE, Mubiru D, Fine RL, Sterpka J, Greiling TM, et al. A diet-sensitive commensal lactobacillus strain mediates TLR7-dependent systemic autoimmunity. *Cell Host Microbe*. 2019;25:113–127. e6. doi:10.1016/j.chom.2018.11.009.
- Vieira SM, Hiltensperger M, Kumar V, Zegarra-Ruiz D, Dehner C, Khan N, Costa FRC, Tiniakou E, Greiling T, Ruff W, et al. Translocation of a gut pathobiont drives autoimmunity in mice and humans. *Science*. 2018;359:1156–1161. doi:10.1126/science.aar7201.
- Thevaranjan N, Puchta A, Schulz C, Naidoo A, Szamosi JC, Verschoor CP, Loukov D, Schenck LP, Jury J, Foley KP, et al. Age-associated microbial dysbiosis promotes intestinal permeability, systemic inflammation, and macrophage dysfunction. *Cell Host*

- Microbe. 2017;21:455–466.e4. doi:10.1016/j.chom.2017.03.002.
27. Medina-Contreras O, Geem D, Laur O, Williams IR, Lira SA, Nusrat A, Parkos CA, Denning TL. CX3CR1 regulates intestinal macrophage homeostasis, bacterial translocation, and colitogenic Th17 responses in mice. *J Clin Investigation*. 2011;121:4787–4795. doi:10.1172/JCI59150.
 28. Zsigmond E, Bernshtein B, Friedlander G, Walker CR, Yona S, Kim K-W, Brenner O, Krauthgamer R, Varol C, Müller W, et al. Macrophage-restricted interleukin-10 receptor deficiency, but not il-10 deficiency, causes severe spontaneous colitis. *Immunity*. 2014;40:720–733. doi:10.1016/j.immuni.2014.03.012.
 29. Kühn R, Löhler J, Rennick D, Rajewsky K, Müller W. Interleukin-10-deficient mice develop chronic enterocolitis. *Cell*. 1993;75:263–274. doi:10.1016/0092-8674(93)80068-P.
 30. Longman RS, Diehl GE, Victorio DA, Huh JR, Galan C, Miraldi ER, Swaminath A, Bonneau R, Scherl EJ, Littman DR. CX₃CR1⁺ mononuclear phagocytes support colitis-associated innate lymphoid cell production of IL-22. *J Exp Medicine* [Internet]. 2014;211:1571–1583. Available from <http://eutils.ncbi.nlm.nih.gov/entrez/eutils/elink.fcgi?dbfrom=pubmed&id=25024136&retmode=ref&cmd=prlinks>.
 31. Jung S, Aliberti J, Graemmel P, Sunshine MJ, Kreutzberg GW, Sher A, Littman DR. Analysis of fractalkine receptor CX(3)CR1 function by targeted deletion and green fluorescent protein reporter gene insertion. *Mol Cell Biol* [Internet]. 2000;20:4106–4114. Available from <http://mcb.asm.org/cgi/doi/10.1128/MCB.20.11.4106-4114.2000>.
 32. Diehl GE, Longman RS, Zhang J-X, Breart B, Galan C, Cuesta A, Schwab SR, Littman DR. Microbiota restricts trafficking of bacteria to mesenteric lymph nodes by CX3CR1hi cells. *Nature* [Internet]. 2013;494:116–120. Available from <http://www.nature.com/doi/10.1038/nature11809>.
 33. Parkhurst CN, Yang G, Ninan I, Savas JN, Yates JR, Lafaille JJ, Hempstead BL, Littman DR, Gan W-B. Microglia promote learning-dependent synapse formation through brain-derived neurotrophic factor. *Cell* [Internet]. 2013;155:1596–1609. Available from. doi:10.1016/j.cell.2013.11.030.
 34. Quiros M, Nishio H, Neumann PA, Siuda D, Brazil JC, Azcutia V, Hilgarth R, O'Leary MN, Garcia-Hernandez V, Leoni G, et al. Macrophage-derived IL-10 mediates mucosal repair by epithelial WISP-1 signaling. *J Clin Investigation*. 2017;127:3510–3520. doi:10.1172/JCI90229.
 35. Werner T, Shkoda A, Haller D. Intestinal epithelial cell proteome in IL-10 deficient mice and il-10 receptor reconstituted epithelial cells: impact on chronic inflammation. *J Proteome Res*. 2007;6:3691–3704. doi:10.1021/pr070222x.
 36. Parang B, Barrett CW, Williams CS. Gastrointestinal Physiology and Diseases. *Methods Mol Biology*. 2016;1422:297–307.
 37. Gonzalez H, Hagerling C, Werb Z. Roles of the immune system in cancer: from tumor initiation to metastatic progression. *Gene Dev*. 2018;32:1267–1284. doi:10.1101/gad.314617.118.
 38. Gabrilovich DI. Myeloid-Derived suppressor cells. *Cancer Immunol Res*. 2017;5:3–8. doi:10.1158/2326-6066.CIR-16-0297.
 39. Ostrand-Rosenberg S, Fenselau C. Myeloid-Derived suppressor cells: immune-suppressive cells that impair antitumor immunity and are sculpted by their environment. *J Immunol Baltim Md 1950*. 2018;200:422–431.
 40. Grivennikov SI, Wang K, Mucida D, Stewart CA, Schnabl B, Jauch D, Taniguchi K, G-Y Y, Osterreicher CH, Hung KE, et al. Adenoma-linked barrier defects and microbial products drive IL-23/IL-17-mediated tumour growth. *Nature*. 2012;491:254–258. doi:10.1038/nature11465.
 41. Mantovani A, Allavena P, Sica A, Balkwill F. Cancer-related inflammation. *Nature*. 2008;454:436–444. doi:10.1038/nature07205.
 42. Zsigmond E, Varol C, Farache J, Elmaliyah E, Satpathy AT, Friedlander G, Mack M, Shpigel N, Boneca IG, Murphy KM, et al. Ly6Chi monocytes in the inflamed colon give rise to proinflammatory effector cells and migratory antigen-presenting cells. *Immunity*. 2012;37:1076–1090. doi:10.1016/j.immuni.2012.08.026.
 43. Wynn TA, Chawla A, Pollard JW. Macrophage biology in development, homeostasis and disease. *Nature*. 2013;496:445–455. doi:10.1038/nature12034.
 44. Kostic AD, Chun E, Robertson L, Glickman JN, Gallini CA, Michaud M, Clancy TE, Chung DC, Lochhead P, Hold GL, et al. *Fusobacterium nucleatum* potentiates intestinal tumorigenesis and modulates the tumor-immune microenvironment. *Cell Host Microbe*. 2013;14:207–215. doi:10.1016/j.chom.2013.07.007.
 45. Dogan B, Suzuki H, Herlekar D, Sartor RB, Campbell BJ, Roberts CL, Stewart K, Scherl EJ, Araz Y, Bitar PP, et al. Inflammation-associated adherent-invasive *Escherichia coli* are enriched in pathways for use of propanediol and iron and M-cell translocation. *Inflamm Bowel Dis*. 2014;20:1919–1932. doi:10.1097/MIB.0000000000000183.
 46. Viladomiu M, Kivolowitz C, Abdulhamid A, Dogan B, Victorio D, Castellanos JG, Woo V, Teng F, Tran NL, Szczesnak A, et al. IgA-coated *E. coli* enriched in Crohn's disease spondyloarthritis promote TH17-dependent inflammation. *Sci Transl Med*. 2017;9:eaaf9655. doi:10.1126/scitranslmed.aaf9655.
 47. Wynn TA, Vannella KM. Macrophages in tissue repair, regeneration, and fibrosis. *Immunity*. 2016;44:450–462. doi:10.1016/j.immuni.2016.02.015.
 48. O'Hara RJ, Greenman J, MacDonald AW, Gaskell KM, Topping KP, Duthie GS, Kerin MJ, Lee PW, Monson JR.

- Advanced colorectal cancer is associated with impaired interleukin 12 and enhanced interleukin 10 production. *Clin Cancer Res Official J Am Assoc Cancer Res.* 1998;4:1943–1948.
49. M-C L, S-H H. IL-10 and its related cytokines for treatment of inflammatory bowel disease. *World J Gastroentero.* 2004;10:620–625. doi:10.3748/wjg.v10.i5.620.
 50. Roers A, Siewe L, Strittmatter E, Deckert M, Schlüter D, Stenzel W, Gruber AD, Krieg T, Rajewsky K, Müller W. T cell-specific inactivation of the interleukin 10 gene in mice results in enhanced T cell responses but normal innate responses to lipopolysaccharide or skin irritation. *J Exp Medicine.* 2004;200:1289–1297. doi:10.1084/jem.20041789.
 51. Pils MC, Pisano F, Fasnacht N, Heinrich J-M, Groebe L, Schippers A, Rozell B, Jack RS, Müller W. Monocytes/macrophages and/or neutrophils are the target of IL-10 in the LPS endotoxemia model. *Eur J Immunol.* 2010;40:443–448.
 52. Buchan A, Hadden M, Suzuki MT. Development and application of quantitative-PCR tools for subgroups of the Roseobacter clade. *Appl Environ Microb* [Internet]. 2009;75:7542–7547. Available from <http://eutils.ncbi.nlm.nih.gov/entrez/eutils/elink.fcgi?dbfrom=pubmed&id=19801463&retmode=ref&cmd=prlinks>.
 53. Chern EC, Siefiring S, Paar J, Doolittle M, Haugland RA. Comparison of quantitative PCR assays for *Escherichia coli* targeting ribosomal RNA and single copy genes. *Lett Appl Microbiol* [Internet]. 2011;52:298–306. Available from <http://eutils.ncbi.nlm.nih.gov/entrez/eutils/elink.fcgi?dbfrom=pubmed&id=21204885&retmode=ref&cmd=prlinks>.
 54. Valdez Y, Diehl GE, Vallance BA, Grassl GA, Guttman JA, Brown NF, Rosenberger CM, Littman DR, Gros P, Finlay BB. Nramp1 expression by dendritic cells modulates inflammatory responses during *Salmonella* Typhimurium infection. *Cell Microbiol* [Internet]. 2008;10:1646–1661. Available from 10.1111/j.1462-5822.2008.01155.x.
 55. Marchal-Bressenot A, Salleron J, Boulagnon-Rombi C, Bastien C, Cahn V, Cadiot G, Diebold M-D, Danese S, Reinisch W, Schreiber S, et al. Development and validation of the Nancy histological index for UC. *Gut.* 2015;66:43–49. doi:10.1136/gutjnl-2015-310187.